# Fabrication and Characterization of Advanced Triple-junction Amorphous Silicon Based Solar Cells

PHASE II – Quarter 2

**Quarterly Technical Progress Report**

June 1, 2006 to August 31, 2006

**NREL Subcontract No.** ZXL-5-44205-06


Subcontractor: The University of Toledo

Principal Investigator: Xunming Deng
(419) 530-4782; dengx@physics.utoledo.edu

Co-Principal Investigator: Robert W. Collins
(419) 530-2195; rcollins@physics.utoledo.edu

Department of Physics and Astronomy
University of Toledo, Toledo, OH 43606

Contract technical monitor: Dr. Bolko von Roedern

## Table of Contents

## Section 1

# Executive Summary

This quarterly technical progress report covers the highlights of the research activities and results on the project of "The Fabrication and Characterization of High-efficiency Triple-junction a-Si Based Solar Cells" at the University of Toledo for the Period of June 1, 2006 to August 31, 2006, under NREL TFPPP subcontract number ZXL-5-44205-06.

Following this Executive Summary are the sections performed during this quarter related to the tasks under this subcontract. The major technical progresses of these sections are summarized as follows:

Section 2: 8% *nc*-Si solar cells deposited over 30 Å/s rate using VHF-PECVD with high pressure high power regime

We examine hydrogenated nanocrystalline silicon (nc-Si:H) cell fabrication under high-rate regime utilizing high pressure high power regime as well as very high frequency technology. Through the optimization of cell deposition condition especially in process pressure, electrode gap, and flow rate of $Si_2H_6$ as well as $H_2$, we accomplished 8.0% efficiency nc-Si:H solar cell with very high deposition rate of 30.4 Å/s. Our external quantum efficiency measurement suggests that the cell efficiency is enabled to push up to 8.6%. We also found that highly crystallized nc-Si:H cell deposited under high-rate can suffer from degradation problem by air exposure because of oxidation of nc-Si:H films. However, appropriate crystal volume fraction around 60% does not provide such kind of degradation. nc-Si:H cell having this value for crystal volume fraction exhibits nice stability against not only air-exposure, but also light-soaking.

Section 3: High deposition rate a-Si(Ge):H solar cells made by VHF-PECVD

Preliminary efforts on the a-Si:H and a-SiGe i-layer depositions were done at high deposition rates around 10 Å/s by using VHF PECVD in the chamber with a new designed showerhead cathode. Both silane and disilane gases have been used alternatively as silicon sources to deposit amorphous silicon and silicon germanium alloy. High quality a-Si:H intrinsic layers were obtained after optimizing the hydrogen dilution, and a-Si:H solar cells show high open-circuit voltages of over 1.0 V. The deposition rates for a-SiGe i-layer preparations are also around 8-10 Å/s. Incorporated with these i-layers, a-SiGe solar cells reached about 8-9% of efficiency under AM1.5G illumination.

Section 4: Surface Roughness and Phase Evolution of Si:H and $Si_{1-x}Ge_x$:H Thin Films Prepared with He Dilution

In this study, the amorphous-phase roughening behavior has been determined as a function of process variables in plasma-enhanced chemical vapor deposition (PECVD) of hydrogenated amorphous silicon-germanium alloys (a-$Si_{1-x}Ge_x$:H). Among the process parameters varied include the $H_2$-dilution gas flow ratio, the $GeH_4$-alloying flow ratio, and the He-dilution flow ratio. One clear feature of this study is a

maximum in the amorphous roughening transition thickness (and hence surface stability) at a $H_2$-dilution ratio just below the transition from amorphous to amorphous+microcrystalline (a+μc) mixed-phase growth irrespective of the other deposition parameters. Additional features of interest involve suppression of the transition to the a+μc mixed phase for alloying with Ge and for diluting the source gases with He.

**Section 2**

# 8% *nc*-Si solar cells deposited over 30 Å/s rate using VHF-PECVD with high pressure high power regime

Yasuaki Ishikawa, Xunming Deng
Department of Physics and Astronomy, University of Toledo, Toledo, OH 43606, USA

## ABSTRACT

We examine hydrogenated nanocrystalline silicon (nc-Si:H) cell fabrication under high-rate regime utilizing high pressure high power regime as well as very high frequency technology. Through the optimization of cell deposition condition especially in process pressure, electrode gap, and flow rate of $Si_2H_6$ as well as $H_2$, we accomplished 8.0% efficiency nc-Si:H solar cell with very high deposition rate of 30.4 Å/s. Our external quantum efficiency measurement suggests that the cell efficiency is enabled to push up to 8.6%. We also found that highly crystallized nc-Si:H cell deposited under high-rate can suffer from degradation problem by air exposure because of oxidation of nc-Si:H films. However, appropriate crystal volume fraction around 60% does not provide such kind of degradation. nc-Si:H cell having this value for crystal volume fraction exhibits pretty nice stability against not only air-exposure, but also light-soaking.

## 1. INTRODUCTION

High rate deposition for hydrogenated nanocrystalline silicon (nc-Si:H) cell fabrication is among the requirements for development of high-efficient multi-junction solar cell in industrial filed. In a bottom component of tandem or triple-junction amorphous silicon based solar cell, it needs around 2 μm thickness or more due to the inherent characteristic for light-absorption. Conventional RF deposition method, using plasma-enhanced chemical vapor deposition (PECVD), enable to deposit device-grade nc-Si:H film with only a few Å/s. Some authors reported the way how to increase a deposition rate for nc-Si:H film formation.

Guo *et al.* initiated nc-Si:H deposition work using high-pressure high-power regime but using RF-PECVD system, and achieved nc-Si:H film deposition with high rate over than 10 Å/s [1]. Several authors introduced VHF (very high frequency) technology into that method. Saito *et al.* developed 10.87% nc-Si:H solar cell (single-junction, nip-type) with 4 Å/s [2], and Mai *et al.* also achieved 10.3% efficiency nc-Si:H solar cell (single-junction, pin-type) with deposition rate of 11 Å/s [3]. AIST (National Institute of Advanced Industrial Science and Technology, Japan) has an initiative for higher rate region, and they recoded 8.2% and 7.9% efficiency (single-junction, pin-type) with 21 Å/s and 30 Å/s, respectively [4]. With nip-type single-junction nc-Si:H solar cell, Neuchâtel Univ. group achieved 7.8% cell with 7.4 Å/s [5], and Uni. Solar group accomplished 8.99% nc-Si:H cell (deposition rate is within 5 ~ 8 Å/s) [6]. Further enhancement of the cell performance under high-rate region is still essential subject in terms of development of multi-junction solar cell in research filed as well as in industrial one.

We examine nc-Si:H film deposition and cell fabrication with this high-pressure high-power regime using VHF plasma excitation. Our objective is as follows: 1) more than 8% efficient cell

with high-rate deposition more than 10 Å/s (that means less than 30min deposition for i-layer process); 2) fabrication of stable nc-Si:H cell for applying multi-junction structure.

## 2. EXPERIMENTAL DETAIL

Capacitive-coupled parallel-plate type PECVD system serves nc-Si:H film on glass, or stainless steel (SS) substrate which is covered by ZnO and Ag. This system has shower-head cathode with 3×3 inch deposition area to realize adequate uniform deposition. The gas mixture of disilane ($Si_2H_6$) and hydrogen ($H_2$) are introduced in the chamber for i-layer deposition. The other doped layers are deposited with different chamber to eliminate cross contamination problem. Silane ($SiH_4$), $H_2$ and phosphine ($PH_3$) gases serve for n-layer, and $SiH_4$, $H_2$ and trifluorobrane ($BF_3$) gases serve for p-layer, respectively. Note that the gases of $Si_2H_6$ and $H_2$ in intrinsic deposition pass through a purifying filter just before controlling the flow rate by mass flow controller, to remove contaminations which are able to come from gas itself and lines. We mount VHF power generator, which is set to 60 or 70 MHz as a plasma excitation frequency, for i-layer deposition, whereas doped layers depositions are carried out with conventional RF plasma.

Table 1 introduces some deposition conditions examined in this study. For i-layer deposition, process pressure less than 2 Torr with electrode gap 15 mm does not enable to excite stable plasma in our chamber configuration. Deposition of nc-Si:H n-layer is performed prior to the deposition of i-layer nc-Si:H absorber, in order to use the n-layer as a seed layer. This n-layer can reduce or remove an incubation layer which is usually formed at the first stage of nc-Si film deposition if one deposited directly on glass or amorphous phase material. Both p and n layer has 15 nm thick, whereas i-layer has 1.4 ~ 2.0 μm

Table 1 Examined deposition condition in this study.

| | Power (W) | Pressure (Torr) | Temp. ($^oC$) | Note |
|---|---|---|---|---|
| n-layer | 100 | 2 | 300 | nc-Si:H |
| i-layer | 60 ~ 100 | 2 ~ 10 | 300 | electrode gap ($d_e$); 7.9 ~ 15 mm |
| p-layer | 3.0 | 0.5 | 300 | - |

After nip deposition on SS with back-reflector (BR), samples receive a deposition of 70 nm thick ITO film by RF magnetron-sputtering method, which also defines the cell area as 0.25$cm^2$, as a front electrode to measure current-voltage (*J-V*) characteristics under AM 1.5 illumination, and external quantum efficiency (EQE) property. The nc-Si:H intrinsic film deposited on top of nc-Si:H n-layer deposited on glass substrates (Corning 1737) provides film thickness by monitoring the step from the edge to the center using a surface-profiler (Dektak3 ST), as well as crystal volume fraction ($X_c$) estimated by Raman scattering spectroscopy with 514.5 nm excitation Ar laser. The $X_c$ is calculated as follows: $X_c = (I_{510}+I_{520}) /(I_{480}+I_{510}+I_{520})$ (%) where $I_{480}$, $I_{510}$ and $I_{520}$ denote integrated intensity at 480, 510 and 520 $cm^{-1}$, respectively, which also correspond the phase fraction of amorphous Si, small crystallite and crystal Si, respectively.

## 3. RESULTS & DISCUSSIONS

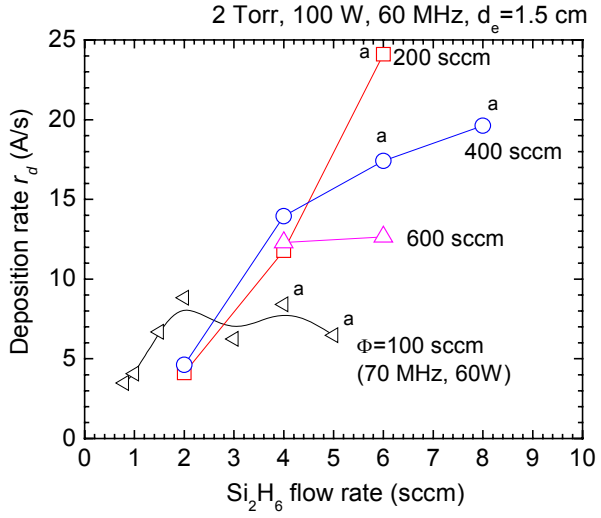


Fig. 1 Deposition rate as a function of $Si_2H_6$ flow rate for several total flow rate. 'a' denotes that the film consists of fully amorphous phase.

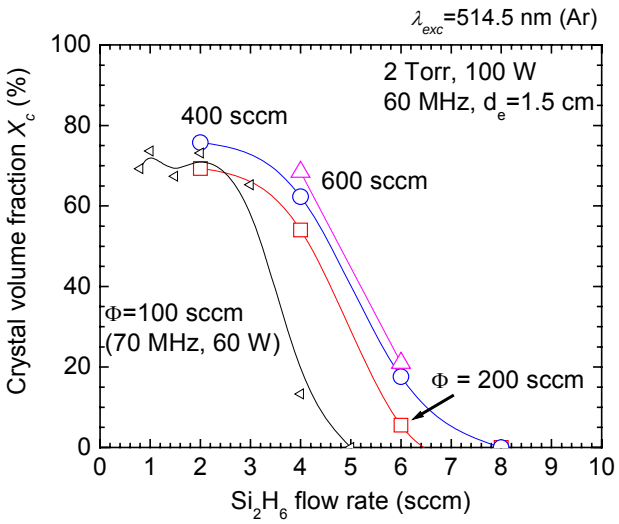


Fig. 2 Crystal volume fraction as a function of $Si_2H_6$ flow rate for several total flow rate cases.

### 3.1 Deposition rate and it crystallinity

nc-Si:H films were deposited on n-layer/glass under high-pressure high-power regime, at first, in order to check the deposition rate as well as the crystal volume fraction in our system. Figure 1 shows the deposition rate as a function of $Si_2H_6$ flow rate for several total flow rate. Except 100 sccm of total flow rate (Φ), films were deposited with 2 Torr, 100 W, 60 MHz and $d_e$ = 15 mm, since higher Φ than 100 sccm did not excite confined plasma effectively between the electrodes with the condition of 60W, 70 MHz.

The deposition rate of nc-Si:H film increases linearly with increasing the $Si_2H_6$ flow rate as shown in Fig. 1. Very high-rate nc-Si:H film more than 30 Å/s, however, was not realized in this condition. Figure 2 displays the crystal volume fraction for deposited samples shown in Fig. 1. At higher total flow rates, the phase transition seems to occur at around 5 or 5.5 sccm of $Si_2H_6$ flow, indicating that the phase transition strongly depends not on the dilution ratio but on the source gas flow rate.

According to the observation of plasma excitation, in $d_e$ = 15 mm condition, we often obtained undesirable plasma excitation surrounding the cathode. However, narrowing the electrode gap to 11 mm successfully excited confined plasma between the electrodes even with 100 sccm of total flow. In below section, we used 11 mm gap, 2 Torr, 100 W, 60 MHz as a standard condition.

### 3.2 Cell performances

We fabricated nc-Si:H solar cell on SS with BR with Φ = 100 sccm and $Si_2H_6$ flow rate = 3.5 ~ 4.5 sccm, which can provide nc-Si:H film having $X_c$ = 30~ 50 % that one can expect to obtain better cell performance in nc-Si:H cell field. Note that the utilized electrode gap in this moment was not 15 mm, but 11 mm. This gap narrowing led in higher $X_c$ value than the case of $d_e$= 15 mm because of allowing higher plasma density between the electrodes. This implied that a shift of the optimum $Si_2H_6$ flow can occur. However, we still obtained the highest efficiency of 4.5 % ($J_{sc}$ = 14.98 mA/cm$^2$, $V_{oc}$ = 0.446 V, $FF$ = 0.671) having 2.0 μm thickness at the flow rate of 3.5

Table 2 Effect of process pressure on cell performances of nc-Si:H solar cell. Electrode gap ($d_e$) was 11 mm, except last two samples. Every cell has a thickness between 1.7 ~ 2.0 μm.

| Pressure (Torr), Power, total flow rate | $J_{sc}$ (mA/cm$^2$) | $V_{oc}$ (V) | *FF* | Effi. (%) | $J_{sc}$(red) (mA/cm$^2$) | $r_d$ (Å/s) |
|---|---|---|---|---|---|---|
| 2 (60W, 100 sccm) | 14.98 | 0.446 | 0.671 | 4.5 | 4.18 | 26.0 |
| 4 (60W, 100 sccm) | 18.64 | 0.488 | 0.691 | 6.3 | 6.36 | 26.1 |
| 6 (60W, 100 sccm) | 12.55 | 0.756 | 0.505 | 4.8 | 3.13 | 29.0 |
| 6 (100W, 100 sccm) | 18.58 | 0.448 | 0.687 | 5.7 | 6.69 | 27.4 |
| 8 (100W, 100 sccm) | 20.25 | 0.440 | 0.683 | 6.1 | 7.60 | 34.7 |
| 8 (100W, 200 sccm) | 20.14 | 0.492 | 0.718 | 7.1 | 7.26 | 38.3 |
| 10 (100W, 200 sccm) | 20.94 | 0.504 | 0.712 | 7.5 | 8.92 | 32.5 |

~ 4.5 sccm. The deposition rate ($r_d$) was around 26 Å/s. Although more precise control for $Si_2H_6$ flow rate allows us to enhance the efficiency and proves that the optimum flow of $Si_2H_6$ is shifted to higher rate, that does not solve essential problem, i.e., still poor $J_{sc}$ value. In next section, we vary the process pressure to see whether enhancement of $J_{sc}$ value is possible or not.

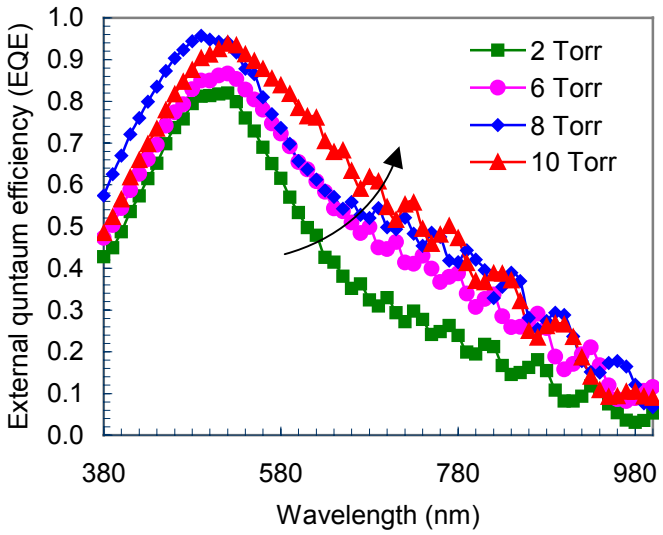


Fig. 3 External quantum efficiency (EQE) spectra for several nc-Si:H solar cells deposited at a pressure of 2, 6, 8, and 10 Torr.

### *3.2.1 Dependence of process pressure*

Table 2 represents that how effective the process pressure is, on enhancement of $J_{sc}$ value. Increasing from 2 Torr to 4 Torr drastically improves $J_{sc}$ as well as $V_{oc}$ value. These two cells were deposited with 60 W. When the pressure increased more than 4 Torr, the plasma became an unstable excitation condition, resulting amorphous phase deposition as shown in Table 2. Higher input power, however, is able to sustain a stable plasma discharge again, led in nc-Si:H formation. We obtained nc-Si:H film again and reached 6.1 % efficiency with 34 Å/s with relatively high red-response of 7.8mA/cm$^2$ which is integrated current density from 650 nm to 1000 nm in EQE measurement. Further increasing of process pressure improves $J_{sc}$ more, and recorded 7.5% efficiency (thickness: 1.7 μm) with over than 32 Å/s deposition rate. Note that the total flow rate was increased to 200 sccm due to improvement of uniformity. In the deposition process between 8 Torr and 10 Torr deposition, we carried out chamber-cleaning, so that the deposition rate dropped from 38 Å/s to 32 Å/s in spite of increase pressure. Note that 10 Torr is the highest controllable pressure in our apparatus. Figure 3 shows some EQE spectra by changing the process pressure. It obviously exhibits that higher pressure achieves higher red-response, especially in 10 Torr case. The total current from EQE spectrum

Table 3 Effect of total flow rate on cell performances of nc-Si:H solar cell. Electrode gap was 9.5mm. Each cell has a thickness around 1.7 μm.

| Total flow rate (sccm), Pressure (Torr) | $J_{sc}$ (mA/cm$^2$) | $V_{oc}$ (V) | *FF* | Effi. (%) | $J_{sc}$(red) (mA/cm$^2$) | $r_d$ (Å/s) |
|---|---|---|---|---|---|---|
| 100, 8 | 20.25 | 0.440 | 0.683 | 6.1 | 7.60 | 34.7 |
| 200, 8 | 20.14 | 0.492 | 0.718 | 7.1 | 7.26 | 38.3 |
| 200, 10 | 20.94 | 0.504 | 0.712 | 7.5 | 8.92 | 32.5 |
| 400, 10 | 20.74 | 0.512 | 0.716 | 7.6 | 8.40 | 32.8 |

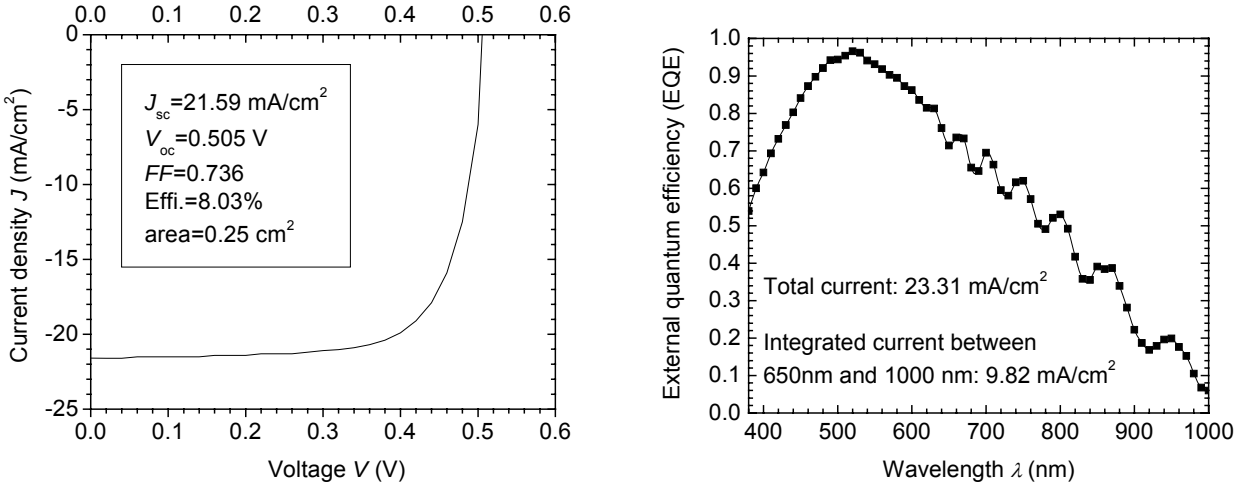


(a) *J-V* (b) EQE

Fig. 4 Current-voltage characteristic (a) and external quantum efficiency (EQE) spectrum (b) of nc-Si:H solar cell with high-rate deposition of 30.4 Å/s.

was estimated as 20.75 mA/cm$^2$ for 10 Torr, when one assumes that the cell received AM1.5 illumination. It indicates that the current is not enough high, although the cell is not applied on highly-textured BR substrate.

### *3.2.2 Impact of total flow rate*

Higher total flow rate enables to drag out higher silane radicals, which are considered to become defect-precursor, i.e., detrimental species for high-quality nc-Si:H film deposition. This method reduces resident time of such kind of precursors, suggesting that one can obtain better cell performances, especially in *FF* and $J_{sc}$. We demonstrated nc-Si:H cell with higher total flow rate as shown in Table 3. *FF* and $J_{sc}$ were gradually improved up to 0.736 and 21.59 mA/cm$^2$, respectively. Consequently, we achieved 8.0% efficiency with 30.4 Å/s deposition rate, by increasing total flow rate as well as process pressure. The current from EQE spectrum was estimated as 23.31 mA/cm$^2$, since our *J-V* simulator is short of red-portion than actual AM1.5 intensity. Therefore, the cell performance can presumably enhance up to 8.6%, if one use $J_{sc}$ from EQE instead of $J_{sc}$ from *J-V* measurement in terms of calculation of cell efficiency. It

should be noted that our BR texturing is not optimized yet, as you can confirm by seeing interference fringes pattern in red-portion in Fig. 4(b). This implies that the cell efficiency still has a room for enhancement.

### *3.2.3 Degradation issue*

We found out a degradation phenomena in nc-Si:H cells having very high $X_c$ contents when the nc-Si:H films are deposited under high-rate. Table 4 exhibits cell performance of initial-state and after two weeks air exposure. With high $X_c$ nc-Si:H cell (a and b), all cell performances received severe degradation, and the degradation rate is gradually reduced with decreasing the $X_c$ value (a→d). When $X_c$ comes to around 60% where we also enable to obtain higher cell performance, no obvious degradation by air exposure is observed. Even in case of very low $X_c$ case (e) as well as amorphous Si cell, no degradation by air exposure occurs. Matsui *et al.* reported that nc-Si:H film, which are deposited at non-optimized condition, can readily oxidize even if the film put in air [7]. Our cell with high $X_c$ has severe deterioration on $V_{oc}$, suggesting the i-layer changes n-type during the two-weeks, since oxygen act as a donor inside of the film. Higher-rate nc-Si:H film might have a lot of void fraction inside, and has a lot of chance to meet donor such as oxygen for strained Si-Si bonds or Si-$H_2$ bonds as well as dangling bonds located around grain boundaries. Further investigation is required in this issue.

Table 4 Comparison of cell performance between the initial state, after air exposure for two weeks and light-soaking (LS) for 100W under AM1.5 illumination with 50°C condition.

| # | state | $V_{oc}$ (V) | $J_{sc}$ (mA/cm$^2$) | *FF* (%) | Effi. (%) | $X_c$ (%) |
|---|---|---|---|---|---|---|
| a | Initial | 0.461 | 22.438 | 0.654 | 6.77 | 74.5 |
| | after 2 weeks | 0.423 | 17.799 | 0.630 | 4.75 | |
| | LS1000 h | 0.387 | 18.805 | 0.588 | 4.28 | |
| b | Initial | 0.456 | 21.980 | 0.690 | 6.91 | 77.3 |
| | after 2 weeks | 0.417 | 18.089 | 0.651 | 4.91 | |
| | LS1000 h | 0.382 | 17.681 | 0.592 | 4.00 | |
| c | Initial | 0.484 | 22.069 | 0.700 | 7.16 | 65.4 |
| | after 2 weeks | 0.464 | 20.885 | 0.687 | 6.66 | |
| | LS1000 h | 0.454 | 20.714 | 0.672 | 6.32 | |
| d | Initial | 0.506 | 21.309 | 0.753 | 8.11 | 60.1 |
| | after 2 weeks | 0.503 | 21.290 | 0.737 | 7.89 | |
| | LS1000 h | 0.510 | 21.92 | 0.722 | 8.07 | |
| e | Initial | 0.564 | 11.359 | 0.532 | 3.41 | amorphous |
| | after 2 weeks | 0.567 | 11.518 | 0.527 | 3.44 | |
| | LS1000 h | 0.557 | 11.692 | 0.485 | 3.16 | |

With light-induced degradation issue, the cell (d) shows very stable characteristics even after 1000 h light-soaking (LS) with AM1.5 illumination at 50°C. Figure 5 shows *J-V* characteristics for initial and 1000 h LS-state of sample (d). $J_{sc}$ and $V_{oc}$ values exhibit slight increase, but *FF* shows opposite trend. The $J_{sc}$ difference is assumed to be a fluctuation of measurement. On the

other hand, $V_{oc}$ increasing is happened for another run, so that it is assured that slight phase transition or hydrogen-passivation to grain boundaries during LS occurs in nc-Si:H film [8].

The cells with higher $X_c$ show still poor stability against LS according to Table 4, however we suppose that there still exist oxidation process during the 1000 h LS in such highly $X_c$ nc-Si:H films. In order to fabricate stable nc-Si:H cell with high-rate, we need further investigation, in terms of crystal volume fraction as well as void fraction.

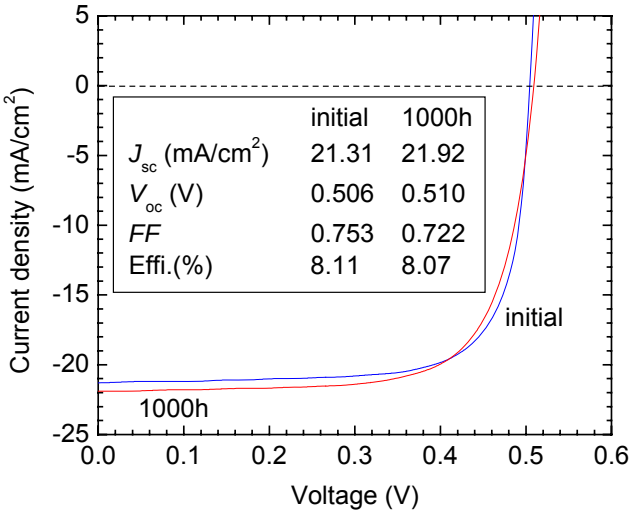


Figure 5 Current-voltage characteristics of initial and light-soaked state (1000 h). The lists of each cell performances are shown in inset of the figure.

## 4. SUMMARY

Optimization of cell deposition conditions for process pressure, electrode gap, and flow rate of $Si_2H_6$ as well as $H_2$ allowed us to accomplish 8.0% efficiency nc-Si:H solar cell with very high deposition rate of 30.4 Å/s. Moreover, EQE measurement supports that the cell efficiency can reached up to around 8.6%. This cell was served on non-optimized back-reflector; therefore there is still open space to enhance the cell performances.

Highly crystallized nc-Si:H cell, which is deposited under high-rate, led in severe degradation problem by air exposure. We assume that this degradation is due to oxidization of nc-Si:H film. It, however, needs further investigation. Low crystal volume fraction does not have this kind of effect, although another degradation such as light induced degradation can occur for nc-Si:H film having low crystal volume fraction. It indicates that appropriate crystal volume fraction exists, in terms of degradation mechanism of not only oxidization but also of light-induced one.

## REFERENCES


1. L. Guo, M. Kondo, F. Fukawa, K. Saitoh, and A. Matsuda, Jpn. J. Appl. Phys. **37** (1998) L1116.
2. K. Saito, M. Sano, A. Sakai, R. Hayashi and K. Ogawa: Tech. Deg. Int. 12th-PVSEC (Jeju, 2001) p-085.
3. Y. Mai, S. Kein, R. Carius, H. Stiebig, X. Geng and F. Finger: Appl. Phys. Lett. 87 (2005) 073503.
4. T. Matsui, M. Kondo and A. Matsuda: WCPEC3 (Osaka, 2003).
5. L. Feitknecht, O. Kluth, Y. Ziegler, X. Niquille, P. Torres, J. Meier, N. Wyrsch and A. Shah: Sol.Ener.Mat.&Sol.Cells 66 (2001) 397-403
6. B. Yan, G. Yue, J.M. Owens, J. Yang, and S. Guha: WCPEC4(Hawaii, 2006)
7. T. Matsui, M. Kondo, and A. Matsuda: Jpn. J. Appl. Phys. **42** (2003) L901.

8. K. Lord, B. Yan, J. Yang, and S. Guha, Appl. Phys. Letts. **79** (2001) 3800.

## Section 3

# High deposition rate a-Si(Ge):H solar cells made by VHF-PECVD

Wenhui Du, Xinmin Cao, Xianbo Liao, Xunming Deng
Department of Physics and Astronomy, University of Toledo, Toledo, OH 43606, USA

### Abstract

Both silane and disilane gases have been used alternatively as silicon sources to deposit amorphous silicon and silicon germanium alloy by Very High Frequency (VHF) Plasma Enhanced Chemical Vapor Deposition (PECVD). High quality a-Si:H intrinsic layers were obtained by optimizing the hydrogen dilution, and a-Si:H solar cells show high open-circuit voltages of over 1.0 V. Germane was then introduced in the process of i-layer deposition. The deposition rates for a-SiGe i-layer preparations are around 8-10 Å/s. Incorporated with these i-layers, a-SiGe solar cells reach about 8 -9% of efficiency under AM1.5G illumination.

### Introduction

Earlier studies by Deng *et al*. [1, 2] have shown that by using VHF PECVD technique and careful selection of deposition conditions, the deposition rate of a-Si:H i-layers could be increased to ~10 Å/s without an observable deterioration in the film and cell properties. The initial and stable cell efficiencies for a-Si solar cells could be made to remain relatively constant with a-Si i-layer deposition rate up to 10 Å/s.

At the University of Toledo (UT), we investigated a-Si:H and a-SiGe intrinsic layers deposited at high deposition rates of ~10 Å/s using our UT multi-chamber load-locked PECVD deposition system with VHF PECVD at a frequency of 60-70 MHz. We adjusted the $H_2$ dilution to deposit material in the amorphous phase close to the transition region, in order to obtain comparable IV results to those of RF-PECVD solar cells, but with a higher deposition rate.

### Experimental details

Using PECVD techniques in our UT multi-chamber load-locked deposition system, a-Si:H and a-SiGe solar cells with n-i-p single-junction structure were fabricated on bare stainless steel (SS) substrates or SS coated with Ag/ZnO back reflectors. The doped n-layers and the doped p-layers were prepared using the conventional 13.56 MHz RF-PECVD technique at a deposition rate of 1 Å/s under the amorphous silicon growth condition, and protocrystalline silicon growth condition, respectively. Using the VHF-PECVD technique with VHF plasma density in the range of 0.2~0.7 W/cm$^2$ and a frequency of 60 MHz or 70 MHz, a-Si and a-SiGe i-layers were fabricated at high deposition rates of about 10 Å/s. Film deposition rate was derived from the reflectance spectrum of film on bare stainless steel. A showerhead cathode was used in the i-layer chamber to improve the film uniformity. $SiH_4/GeH_4$ mixture as well as $Si_2H_6/GeH_4$ mixture were used to

grow SiGe alloy for comparison. The substrate temperature is in the range of 200 – 400 °C. High hydrogen dilution was used for i-layer deposition. After fabrication of the n-i-p single-junction structure, the cells were completed with a mask by depositing Indium Tin Oxides (ITO) transparent conductive layers as front contacts using standard RF magnetron-sputtering deposition techniques. Each cell has an active area of 0.25 $cm^2$. For characterization of the as-deposited cells, standard AM1.5G light current-voltage (I-V) and dark I-V measurements were made. Standard QE measurements were also made in the wavelength range of 350 – 1000nm.

**Results and Discussions**

**1. a-Si:H solar cells with i-layer made using $SiH_4/H_2$ mixture**

Preliminary effort on the a-Si:H i-layer deposition was done at deposition rates around 10 Å/s by using VHF PECVD and $SiH_4/H_2$ mixture in the chamber with a showerhead cathode. The hydrogen dilution ratio of R = $[H_2]/[SiH_4]$ was increased from 9 to 20 during the i-layer deposition. In the previous study, we have shown that the standard top component a-Si:H solar cell has the best open-circuit voltage when the R = $[H_2]/[Si_2H_6]$ ratio is about 100. The optimized dilution ratio in case of using $SiH_4$ is much smaller than that using $Si_2H_6$. It can be seen from Table 1 that the R = $[H_2]/[SiH_4]$ = 12 solar cell has the highest open-circuit voltage of 0.980V and the best efficiency of 5.06%. Material obtained using a lower R is expected to be poor amorphous structure and higher R contains nano-structures. Deposition rate is about 8-9 Å/S when R is around 12.

Table 1. I-V parameters of a-Si:H solar cells as function of R = $[H_2]/[SiH_4]$ during the i-layer deposition, p being 0.6 Torr and Ts 200C.

| Sample # | R | Voc (V) | Jsc ($mA/cm^2$) | FF (%) | Eff (%) | $R_d$ (Å/s) |
|---|---|---|---|---|---|---|
| GD1809 | 9 | 0.975 | 7.63 | 66.7 | 4.96 | 10 |
| GD1810 | 12 | 0.980 | 7.84 | 65.9 | 5.06 | 8 |
| GD1819 | 15 | 0.935 | 8.75 | 58.7 | 4.80 | 9 |
| GD1822 | 20 | 0.792 | 6.58 | 64.2 | 3.35 | 14 |

**2. a-Si:H solar cells with i-layer made using $Si_2H_6/H_2$ mixture**

Preliminary effort on the a-Si:H i-layer deposition was also done at deposition rates around 8 Å/s by using $Si_2H_6/H_2$ mixture in the showerhead chamber. The best Voc values around 1.03V were

obtained for solar cells made under R = 80 ~100. Optimized hydrogen dilution values as function of pressure were also studied and listed in Table 2. It seems that at high pressure, either hydrogen dilution or plasma power needs to be adjusted. At 4 Torr, the hydrogen dilution was reduced to 30 from 100 at 0.6 Torr. In order to clarify the influence of deposition pressure and plasma power on the amorphous phase formation, series of samples have been done at 10 Torr, as displayed in Table 3. High power is preferable to induce nanocrystalline in the films even using a very low hydrogen dilution ratio of 30 where the corresponding $V_{oc}$ is around 0.461V. The second series of sample were made at constant hydrogen dilution ratio of 30, with gradually reduced power. When the power was reduced from 100W to 75 W, the Voc changes dramatically from 0.46V to 0.98V. It shows materials enter the amorphous phase region when grown in 50 to 75W region. The plasma power lower than 50 W causes more defected structure in i-layers, which induce the poor fill factors.

Table 2 High rate a-Si:H solar cell made at different pressure

| Pressure (Torr) | Cell # | $H_2$ dilution R | $V_{oc}$ (V) | $J_{sc}$ (mA/cm | FF (%) | Eff (%) | $R_d$ (Å/s) |
|---|---|---|---|---|---|---|---|
| 0.6 | GD1779 | 100 | 1.028 | 6.9 | 72.2 | 5.1 | 5 |
| | GD1786 | 80 | 1.032 | 7.0 | 71.0 | 5.1 | 8 |
| 2 | GD2036* | 10 | 1.01 | 11.5 | 67.4 | 7.8 | 6 |
| | GD2039* | 10 | 0.963 | 12.0 | 71.3 | 8.3 | 9 |
| | GD2101 | 100 | 1.001 | 10.6 | 71.5 | 7.6 | 10 |
| | GD2112 | 100 | 0.998 | 12.6 | 66. 8 | 8.4 | 10 |
| 4 | GD2066 | 40 | 0.946 | 12.5 | 60.8 | 7.2 | 9 |
| | GD2067 | 30 | 0.990 | 11.2 | 68.1 | 7.6 | 9 |

( * SiH4 is served as Si sources)

Table 3 I-V parameters of a-Si:H solar cells made under different $H_2$ dilution R and power settings

| sample no | $H_2$ dilution R | power (W) | $R_d$ (Å/s) | Voc (V) | Jsc ($mA/cm^2$) | FF | Eff (%) |
|---|---|---|---|---|---|---|---|
| GD2131 | 75 | 100 | 3.6 | 0.424 | 12.0 | 0.70 | 3.6 |
| GD2134 | 50 | 100 | 6.3 | 0.424 | 12.2 | 0.70 | 3.6 |
| GD2132 | 30 | 100 | 8.2 | 0.461 | 16.5 | 0.68 | 5.2 |
| GD2133 | 30 | 75 | 8.8 | 0.982 | 15.2 | 0.58 | 8.6 |
| GD2143 | 30 | 50 | 9.0 | 0.989 | 14.0 | 0.53 | 7.3 |
| GD2144 | 30 | 25 | 10 | 0.901 | 8.7 | 0.31 | 2.4 |
| GD2145 | 20 | 50 | 13 | 0.947 | 5.7 | 0.22 | 1.2 |

### 3. I-V results of a-SiGe solar cells

Based on the optimized deposition for high quality a-Si:H intrinsic layers made by using VHF PECVD and $SiH_4/H_2$ mixture, Germane was then introduced in the process of a-SiGe i-layer deposition. The deposition rates for a-SiGe i-layer preparations are around 8-10 Å/s. Incorporated with these i-layers, a-SiGe solar cells reach about 8-9% of efficiency under AM1.5G illumination. Table 4 lists IV results of 3 samples made with different $GeH_4/SiH_4$ and $H_2/SiH_4$ ratio in the i-layer deposition. VHF- cells have smaller short-circuit current, and the loss is caused by the red photons contribution. Another issue need be concerned is that the difference in open-circuit voltage between the centre cell and edge cell. Even using showerhead cathode design, the edge cell has a better voltage. The reason is investigated by modifying cathode design.

Table 4. IV results of a-SiGe:H solar cells made using $SiH_4$ and $GeH_4$ mixture

| Cell # | Rd (A/s) | d (nm) | $V_{oc}$ (V) | $J_{sc}$ (mA/cm2) | FF (%) | EFF (%) | note |
|---|---|---|---|---|---|---|---|
| GD1867 | 9.5 | 220 | 0.648 | 20.30 | 69.7 | 9.20 | centre |
| | | | 0.664 | 19.90 | 65.4 | 8.60 | edge |
| GD1877 | 11 | 210 | 0.629 | 19.06 | 63.2 | 7.56 | Higher Ge/Si ratio |
| GD1878 | 8.5 | 210 | 0.643 | 19.99 | 62.2 | 7.99 | Higher R & Ge/Si ratio |

## Summary

a-Si to nc-Si phase transition happens at R ($H_2/SiH_4$) ~12, the best solar cell $V_{oc}$ is around 1.01 V at $R_d$~9 Å/s. Solar cells present about 1.03 V of Voc when it was made by VHF-PECVD at $R_d$= 8 Å/s. At high pressure and high plasma power region, high quality a-Si i-layers can be obtained at high eposition rate, ~ 10 Å/S.

a-SiGe intrinsic layer were deposited at $R_d$ ~10 Å/sec with solar cell efficiency around 8-9% for using either $SiH_4$ or $Si_2H_6$ gases as Si sources. Film uniformity is another key issue for a-SiGe alloy deposition. It is found centre cells have a lower $V_{oc}$ than the edge cells at a certain power. The cause is being studied by changing the cathode design.

## References

[1] X. Deng, S.J. Jones, T. Liu, M. Izu, S.R. Ovshinsky and K. Hoffman, "VHF plasma deposition of high performance microcrystalline silicon p-layer materials", in *Amorphous and Microcrystalline Silicon Technology--1997*, edited by E.A. Schiff, M. Hack, S. Wagner, R. Schropp, and I. Shimizu (Materials Research Society, Pittsburgh, 1997), Vol. **467**, p.795.

[2] X. Deng, S.J. Jones, T. Liu, M. Izu and S.R. Ovshinsky, "Improved μc-Si p-layer and a-Si i-layer materials using VHF plasma deposition", in *Conference Record of the Twenty Sixth IEEE Photovoltaic Specialists Conference--1997*, p.591 (1997).

## Section 4

# Surface Roughness and Phase Evolution of Si:H and $Si_{1-x}Ge_x$:H Thin Films Prepared with He Dilution

N. J. Podraza and R. W. Collins

Department of Physics and Astronomy, the University of Toledo, Toledo, OH 43606, USA

## Overview

In this study, the amorphous-phase roughening behavior has been determined as a function of process variables in plasma-enhanced chemical vapor deposition (PECVD) of hydrogenated amorphous silicon-germanium alloys (a-$Si_{1-x}Ge_x$:H). Among the process parameters varied include the $H_2$-dilution gas flow ratio, the $GeH_4$-alloying flow ratio, and the He-dilution flow ratio. One clear feature of this study is a maximum in the amorphous roughening transition thickness (and hence surface stability) at a $H_2$-dilution ratio just below the transition from amorphous to amorphous+microcrystalline (a+μc) mixed-phase growth irrespective of the other deposition parameters. Additional features of interest involve suppression of the transition to the a+μc mixed phase for alloying with Ge and for diluting the source gases with He.

## 1. Introduction

Extensive research on hydrogenated amorphous silicon (a-Si:H) thin films has shown that optimum device performance is correlated with the smoothest, most stable surfaces versus time during the PECVD process – in fact, less than a monolayer of roughening occurs throughout the deposition of optimum films as thick as 0.5 μm [1]. Such research requires smooth crystalline silicon substrates for high sensitivity to the surface roughness evolution as well as an in situ probe such as spectroscopic ellipsometry (SE) for real-time analysis. It has been also shown that when the PECVD conditions deviate from the optimum even slightly, e.g., by a reduction in the hydrogen dilution ratio or by an increase in plasma power from the minimum possible, then a roughening transition is observed in the a-Si:H growth regime. This transition shifts to decreasing bulk layer thickness for films with increasingly deteriorated device properties. As a result, the thickness at which the roughening transition (denoted a $\rightarrow$ a) occurs has been entered into deposition phase diagrams, relevant for c-Si substrates, that provide insights into the device quality of a-Si:H and how it varies with deposition parameters. In the present study, the roughening transition has been characterized versus deposition parameter variations for PECVD a-$Si_{1-x}Ge_x$:H, an alloy that has traditionally posed considerable optimization challenges.

## 2. Experimental Details

The $Si_{1-x}Ge_x$:H films in this study were deposited onto native-oxide/c-Si substrates using single-chamber rf (13.56 MHz) PECVD and were measured in real time using a rotating-compensator multichannel ellipsometer [2]. The fixed parameters were selected for the most part at values used in previous studies of pure Si:H PECVD [1], including a relatively low substrate temperature (T = 200°C), the minimum rf power for plasma stability (P ~ 0.08 W/cm$^2$), a low partial pressure of the source gases {[$SiH_4$]+[$GeH_4$]} ($p_{par}$ ~ 0.06 Torr), and a low total pressure ($p_{tot}$ < 1.0 Torr). In this study, the primary phase diagram variable was the $H_2$-dilution ratio R = [$H_2$] /{[$SiH_4$]+[$GeH_4$]}, as usual. The other variable parameters unique to the $Si_{1-x}Ge_x$:H deposition include the alloying flow ratio G = [$GeH_4$]/{[$SiH_4$]+[$GeH_4$]} which was varied from G = 0 to G = 0.167, leading to x values up to 0.4 and He-dilution defined by the flow ratio He=[He]/{[$SiH_4$]+[$GeH_4$]}which was varied from 0 to 90. The optical gap of the a-$Si_{1-x}Ge_x$:H reached its minimum of ~1.3 eV for the maximum G value, with smaller variations due to the other parameters.

## 3. Results and Discussion

Figures 1-3 provide a comparison between the roles of $H_2$ and He-dilution for $Si_{1-x}Ge_x$:H alloys (G=0.167) prepared by standard anode PECVD and explore the possibility that He dilution can improve the properties of these alloys.

Figure 1 shows the surface roughness evolution for a film prepared with R = 80 without He-dilution. Under these conditions the a $\rightarrow$ a and a $\rightarrow$ (a+μc) transitions occur near bulk layer thicknesses of 200 and 800 Å, respectively. The low value of the former transition thickness is an indication of a short precursor diffusion length on the film surface and poor electronic properties in spite of the proximity to the a $\rightarrow$ (a+μc) transition. Figure 1 also includes the roughness evolution of a film prepared with R=80 and He = [He] /{[$SiH_4$]+[$GeH_4$]} = 20. In this case, the addition of He shifts the a $\rightarrow$(a+μc) transition to higher R such that the film remains amorphous throughout deposition. Furthermore the a $\rightarrow$ a transition thickness shifts to somewhat higher values, but not nearly as much as occurs with the change in electrode configuration from anode to cathode as described in previous studies [3]. The significance of this shift is that under all observed deposition conditions the a $\rightarrow$ a transition thickness is maximized just before the thick film a $\rightarrow$ (a+μc) transition [1]. This indicates that under all conditions, the precursor surface diffusion length [4,5] and ultimately electronic quality [6] improve together with increasing R, right up to the a $\rightarrow$ (a+μc) transition for the desired thickness. In fact previous RTSE studies have identified direct correlations between the a $\rightarrow$ a transition and the precursor surface diffusion length [7], as well as dielectric function parameter shifts versus R [8], indicating improved electronic film quality.

Figure 2 summarizes all results for deposition rate versus the combined [$H_2$+He]-dilution ratio S = R+He = {[$H_2$]+[He]} / {[$SiH_4$]+[$GeH_4$]}. Here, results for the nine depositions without He-dilution are plotted, along with two sets of depositions, one in which R=10 and the dominant dilution effect is He (four depositions with He increasing from 0 to 90), and the other in which R=80 and the dominant dilution effect is $H_2$ (two depositions with He = 0, 20). Figure 3 shows the phase diagrams for the same sets of samples. The following observations can be made.

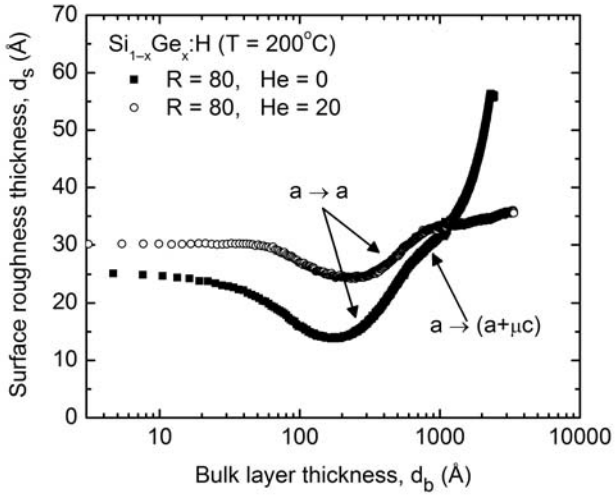


**Fig. 1:** Surface roughness evolution for two $Si_{1-x}Ge_x$:H films prepared in the anode configuration with R = $[H_2]/\{[SiH_4]+[GeH_4]\}$ = 80 and G = $[GeH_4]/\{[SiH_4]+[GeH_4]\}$ = 0.167. One film was prepared with He = $[He]/\{[SiH_4]+[GeH_4]\}$ = 0 and the other with He = 20.

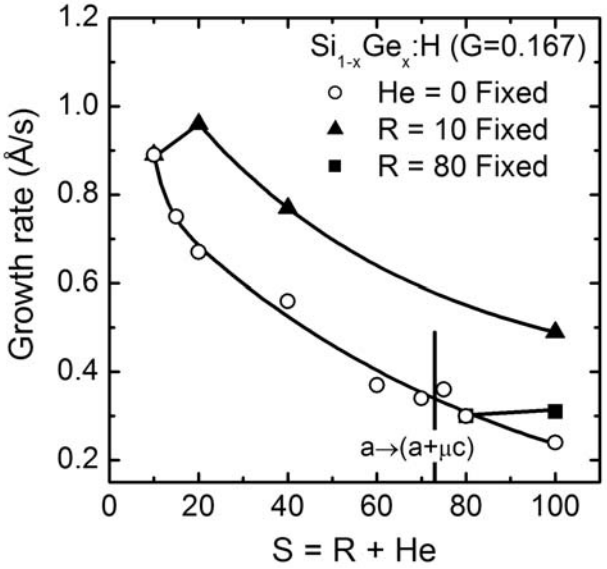


**Fig. 2:** Deposition rate versus the combined $[H_2]$+[He]-dilution ratio S = R + He = $\{[H_2] + [He]\}/\{[SiH_4] + [GeH_4]\}$ for $Si_{1-x}Ge_x$:H films prepared in the anode configuration with G = $[GeH_4]/\{[SiH_4] + [GeH_4]\}$ = 0.167. Here, results for the nine depositions without He-dilution are plotted along with two series of depositions, one in which R is fixed at 10 and the dominant dilution effect is He (four depositions with He increasing from 0 to 90), and the other in which R is fixed at 80 and the dominant dilution effect is $H_2$ (two depositions with He = 0, 20).

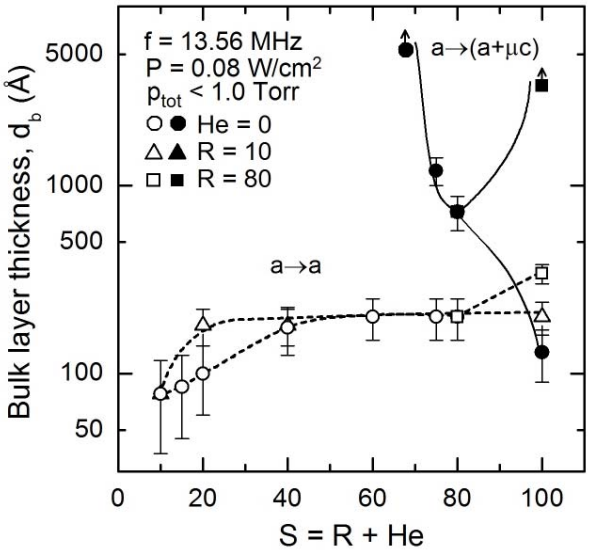


**Fig. 3:** Deposition phase diagrams plotted versus the combined $[H_2 + He]$-dilution ratio S = R + He = $\{[H_2] + [He]\}$ /$\{[SiH_4] + [GeH_4]\}$ for the $Si_{1-x}Ge_x$:H film set of Fig. 2, prepared in the anode configuration with G = $[GeH_4]$ / $\{[SiH_4] + [GeH_4]\}$ = 0.167. The broken lines denote the a → a transitions while the solid lines denote the a → (a+μc) transitions.

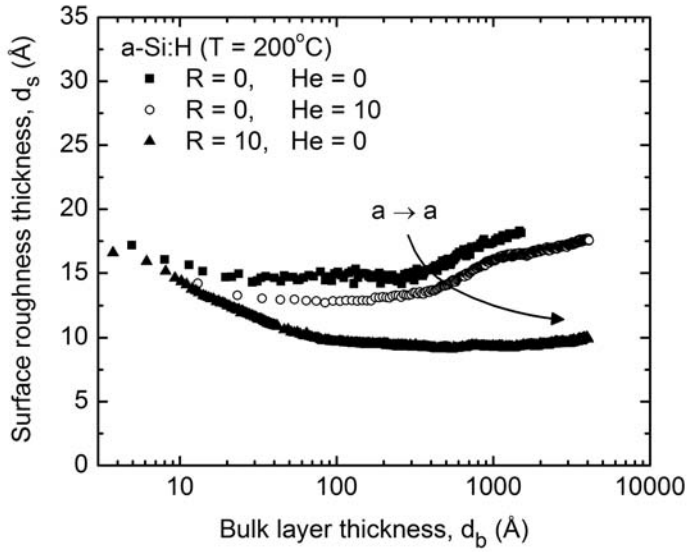


**Fig. 4:** Surface roughness evolution for three a-Si:H films prepared by rf PECVD, f = 13.56 MHz, in the anode configuration with a substrate temperature T = 200°C, plasma power P=0.08 W/cm$^2$, a low total pressure of $p_{tot}$ < 1 Torr, and with i) R = $[H_2]/[SiH_4]$ = 0, He = $[He]/[SiH_4]$ = 0 (squares); ii) R = 0, He = 10 (circles); and iii) R = 10, He = 0 (triangles).

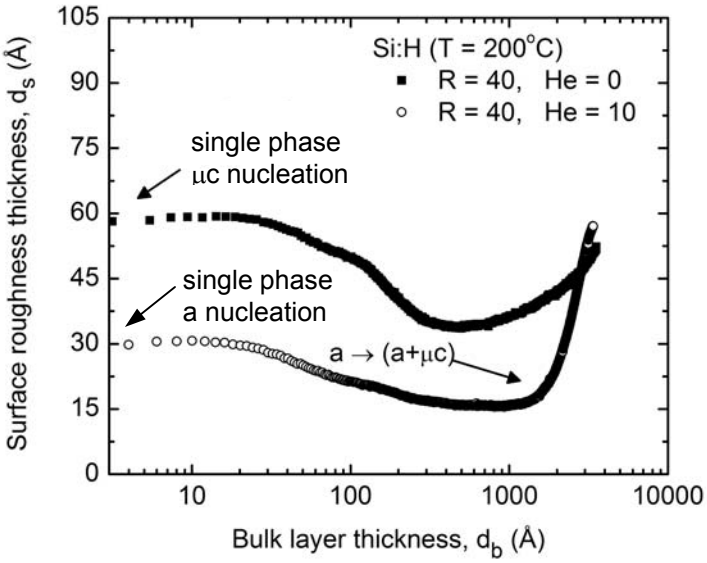


**Fig. 5:** Surface roughness evolution for two Si:H films prepared by rf PECVD, f = 13.56 MHz, in the anode configuration with a substrate temperature T = 200°C, plasma power P=0.08 W/cm$^2$, a low total pressure of p < 1 Torr, and with (i) R=$[H_2]/[SiH_4]$=40, He=$[He]/[SiH_4]$=0 (squares) and (ii) R=40, He=10 (circles).

(i) Dominant $H_2$-dilution (He=0) and He dilution (R=10) generate similar a $\rightarrow$ a transition thicknesses, even though higher deposition rates are achieved with dominant He dilution. (ii) A larger a $\rightarrow$ a transition thickness and improved properties are possible (without sacrificing rate) by using He-dilution to suppress the a $\rightarrow$ (a+μc) transition, enabling a larger R value, as shown for the deposition with R=80 and He=20 in Figs. 1 and 3. The larger amplitude of $d_s$ for this deposition in Fig. 1 appears to be due to a lower nucleation density, possibly a result of longer precursor diffusion length on the substrate surface.

Similarly, Figures 4 and 5 show the effects of He dilution observed for $Si_{1-x}Ge_x$:H are also evident for Si:H. Figure 4 shows the surface roughness evolution of three depositions prepared with no dilution (R=0, He=0); hydrogen dilution only (R=10, He=0); and helium dilution only (R=0, He=10). This figure demonstrates that although He=10 dilution can be used to shift the a $\rightarrow$ a roughening transition from $d_b$ = 220 Å to $d_b$ = 400 Å, thereby increasing precursor diffusion length on the surface and improving film quality, the effect fails to reach improvement gained by $H_2$ dilution (R=10) alone where the a $\rightarrow$ a roughening transition occurs at $d_b$ > 4000 Å. Figure 5 demonstrates the effect of He dilution on Si:H growth along with $H_2$ dilution conditions (R=40). The film prepared at He=0, R=40 shows immediate single phase microcrystallite nucleation. In contrast, the corresponding He diluted film prepared at He=10, R=40 exhibits immediate single phase amorphous nucleation and a mixed phase amorphous plus microcrystalline [a $\rightarrow$ (a+μc)] transition at $d_b$ = 1400 Å. This effect demonstrates that He dilution suppresses microcrystallite formation in both a-$Si_{1-x}Ge_x$:H and a-Si:H materials. This suppression of microcrystallinity can be used to create an extended protocrystalline regime at higher $H_2$ dilution ratio R.

## 5. Summary

Surface roughness evolution has been studied and phase diagrams have been developed for Si:H and $Si_{1-x}Ge_x$:H films prepared with and without helium dilution in order to explore the role of low-energy ion bombardment from plasma-excited He. He dilution for $Si_{1-x}Ge_x$:H anode films shifts the thick-film a $\rightarrow$ (a+μc) transition to higher R; however, in the uncovered regime in R, the a $\rightarrow$ a roughening transition shifts only slightly to higher bulk layer thicknesses, a much weaker effect than occurs under other low-energy ion bombardment conditions, for example, cathodic deposition [3]. Similarly, Si:H anode films prepared under He dilution also demonstrate a modest improvement in film quality, as indicated by higher bulk layer thicknesses at which the a $\rightarrow$ a roughening transition saturates. This improvement, however, is weaker than that achieved by $H_2$ dilution alone. Additionally, He dilution of high-R Si:H films have been shown to suppress microcrystallite formation, thereby shifting the a $\rightarrow$ (a+μc) transition to higher bulk layer thicknesses, opening up an extended protocrystalline regime for films undergoing mixed phase and single phase microcrystalline transitions.

**Acknowledgments**

This research was supported by NREL (Subcontract Nos. NDJ-1-30630-01 and ZXL-5-44205-06).

## References


[1] R.W. Collins, A.S. Ferlauto, G.M. Ferreira, C. Chen, J. Koh, R. Koval, Y. Lee, J.M. Pearce, and C.R. Wronski, *Solar Energy Mater. Solar Cells* **78**, 143 (2003).

[2] I. An, J.A. Zapien, C. Chen, A.S. Ferlauto, A.S. Lawrence, and R.W. Collins, *Thin Solid Films* **455**, 132 (2004).

[3] N.J. Podraza, C.R. Wronski, M.W. Horn, and R.W. Collins, *Mater. Res. Soc. Symp. Proc.* **910**, A.03.2.1-6 (2006).

[4] A. Mazor, D.J. Srolovitz, P.S. Hagan, and B.G. Bukiet, *Phys. Rev. Lett.* **60**, 424 (1988).

[5] R.S. Williams, W.M. Tong, and T.T. Ngo, *Mater. Res. Soc. Symp. Proc.* **367**, 273 (1995).

[6] G. Ganguly and A. Matsuda, *Phys. Rev.* B **47**, 3661 (1993).

[7] N.J. Podraza, C.R. Wronski, and R.W. Collins, *J. Non-Cryst. Solid,* **352**, 950 (2006).

[8] N.J. Podraza, C.R. Wronski, M.W. Horn, and R.W. Collins, *Mater. Res. Soc. Symp. Proc.* **910**, A.10.1.1-6 (2006).